PROCEEDINGS OF SPIE

SPIEDigitalLibrary.org/conference-proceedings-of-spie

Spectral illumination system utilizing spherical reflection optics

Gunn Mayes, Samantha, Browning, Craig, Mayes, Samuel, Parker, Marina, Rich, Thomas, et al.

Samantha Gunn Mayes, Craig Browning, Samuel A. Mayes, Marina Parker, Thomas C. Rich, Silas J. Leavesley, "Spectral illumination system utilizing spherical reflection optics," Proc. SPIE 11243, Imaging, Manipulation, and Analysis of Biomolecules, Cells, and Tissues XVIII, 112430L (17 February 2020); doi: 10.1117/12.2546395

SPIE.

Event: SPIE BiOS, 2020, San Francisco, California, United States

Downloaded From: https://www.spiedigitallibrary.org/conference-proceedings-of-spie on 16 Mar 2020 Terms of Use: https://www.spiedigitallibrary.org/terms-of-use

Spectral Illumination System Utilizing Spherical Reflection Optics

Samantha Gunn Mayes[1], Craig Browning[1,4], Samuel A. Mayes[1,4], Marina Parker[1,4], Thomas C.Rich[2,3], Silas J. Leavesley[1,2,3]

[1]Department of Chemical and Biomolecular Engineering, [2]Department of Pharmacology, [3]Center for Lung Biology, University of South Alabama, [4]Department of Systems Engineering

ABSTRACT

Fluorescence imaging microscopy has traditionally been used because of the high specificity that is achievable through fluorescence labeling techniques and optical filtering. When combined with spectral imaging technologies, fluorescence microscopy can allow for quantitative identification of multiple fluorescent labels. We are working to develop a new approach for spectral imaging that samples the fluorescence excitation spectrum and may provide increased signal strength. The enhanced signal strength may be used to provide increased spectral sensitivity and spectral, spatial, and temporal sampling capabilities. A proof of concept excitation scanning system has shown over 10-fold increase in signal to noise ratio compared to emission scanning hyperspectral imaging. Traditional hyperspectral imaging fluorescence microscopy methods often require minutes of acquisition time. We are developing a new configuration that utilizes solid state LEDs to combine multiple illumination wavelengths in a 2-mirror assembly to overcome the temporal limitations of traditional hyperspectral imaging. We have previously reported on the theoretical performance of some of the aspects of this system by using optical ray trace modeling. Here, we present results from prototyping and benchtop testing of the system, including assembly, optical characterization, and data collection. This work required the assembly and characterization of a novel excitation scanning hyperspectral microscopy system, containing 12 LEDs ranging from 365-425 nm, 12 lenses, a spherical mirror, and a flat mirror. This unique approach may reduce the long image acquisition times seen in traditional hyperspectral imaging while maintaining high specificity and sensitivity for multilabel identification and autofluorescence imaging in real time.

Keywords: Spectral, Spectroscopy, Fluorescence, Microscope, Microscopy, Imaging, Bioimaging, HSI

1.0 INTRODUCTION

Currently, fluorescence imaging uses labeling and optical filtering to visualize molecular structures and activity. Fluorescent labels are typically detected at their peak wavelengths and allow for specific imaging of one or more of the labels .[12] Hyperspectral imaging (HSI) expands on this concept by collecting contiguous spectral data at each pixel.[3–6] Normally, HSI systems separate the emitted fluorescence into different spectral bands using one of many approaches for spectral filtering or dispersion.[3,7–9] These systems often have tradeoffs in acquisition time, specificity, and sensitivity.

Our current work is to develop an excitation scanning system to overcome tradeoffs seen in traditional HSI. In this system we combine a pair of beam splitting mirrors and illumination sources over multiple wavelengths to acquire images at faster speeds while maintaining a high signal to noise ratio. In this system, the sample is excited at each band of illumination, and the entire emission spectra above the dichroic beamsplitter cutoff can be detected. The composite image across the entire excitation spectrum provides hyperspectral discrimination.[10–12]

Here, we present results from an initial prototype that was developed from an optimized optical model. The result of bench testing the prototype are compared with the optimization of the optical model. The prototype light source will provide end-user applications in endoscopy and microscopy .[13–16]

Imaging, Manipulation, and Analysis of Biomolecules, Cells, and Tissues XVIII, edited by Daniel L. Farkas, Attila Tarnok,
Proc. of SPIE Vol. 11243, 112430L · © 2020 SPIE · CCC code: 1605-7422/20/$21 · doi: 10.1117/12.2546395

Downloaded From: https://www.spiedigitallibrary.org/conference-proceedings-of-spie on 16 Mar 2020
Terms of Use: https://www.spiedigitallibrary.org/terms-of-use

2.0 METHODS

2.1 Theoretical Optical Model

The optical model was simulated using TracePro software (Lambda Research Corporation). Initial results from the optical modeling were first presented in a Photonics West 2019 proceedings paper and Figures 1-3 are re-presented here for context to allow comparison to the experimental prototype results.[17] This model included a spherical concave mirror, a flat mirror, LEDs, a liquid light guide input, and up to two different lenses as shown in Figure 1. Optimization of this model consisted of maximizing the optical throughput of the LED to the liquid light guide input. This was accomplished by varying different parameters including using two different lens configurations; a configuration with one focusing lens (Figure 1, left) and a configuration with a collimating and a focusing lens (Figure 1, right). Optimization also included changing the focal length of lenses and the concave mirror along with varying the z and x position of both the lenses and LED.

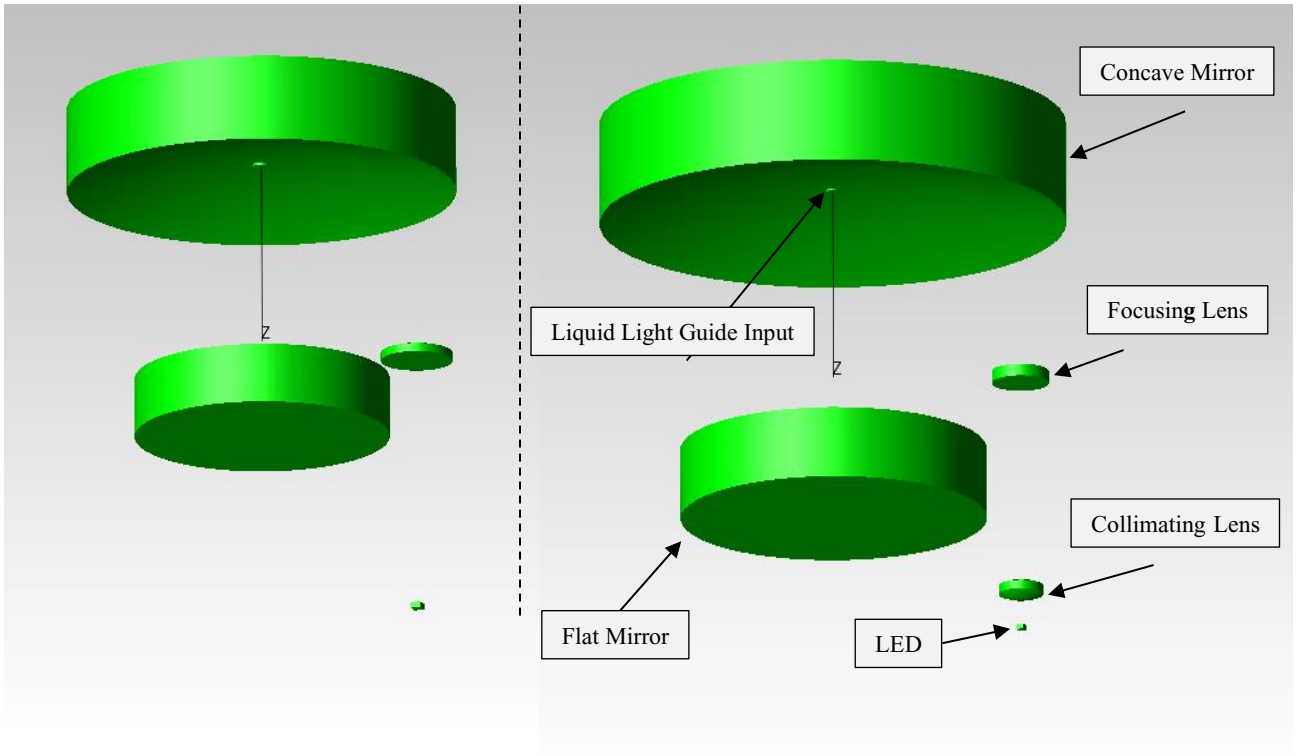

Figure 1 – Initial data is shown here for comparison from the previous year's proceedings paper. A screenshot of the optical ray trace model in Tracepro showing the single lens configuration (left) and a dual lens configuration (right). The single-lens configuration was used for refocusing the emitted light at a distance corresponding to the entrance of the liquid light guide. The dual-lens configuration was used to collimate and then refocus the emitted light at the liquid light guide entrance aperture.[17]

The LED properties were generated in TracePro by importing data from manufacturer's specification sheets. A 525 nm LED with high power output and low dispersion angle was used (part # SMB1N-525V-02, Roitherner LaserTechnik GmbH). This illumination pattern of this LED was assigned to an object in the software model representing the LED and allowed for simulating ray traces, an example of which is shown in Figure 2 (left). In Figure 2, rays are directed from the LED to the center of the concave mirror where the liquid light guide is located. The surface of the liquid light guide is where results were generated through the use of an irradiance map, shown in Figure 2 (right). The results of the optimization suggested a 76.2 mm focal length mirror array using a single 45 mm focal length lens provided maximal illumination onto the surface of the liquid light guide.

Downloaded From: https://www.spiedigitallibrary.org/conference-proceedings-of-spie on 16 Mar 2020
Terms of Use: https://www.spiedigitallibrary.org/terms-of-use

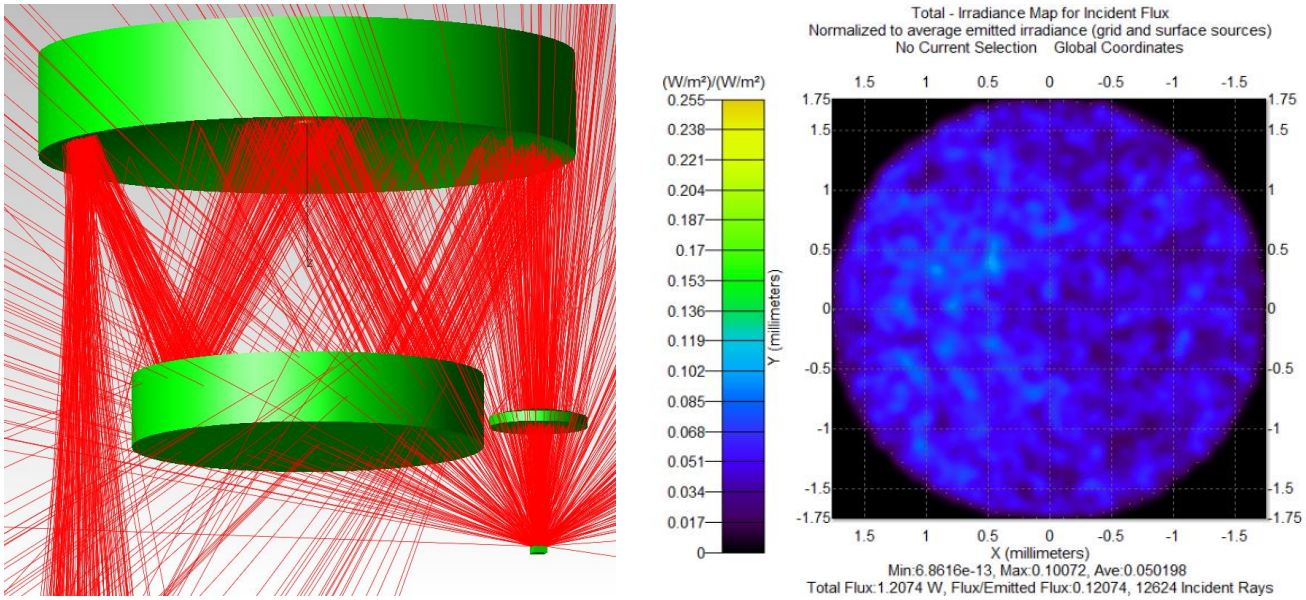

Figure 2 – Initial data is shown here for comparison from the previous year's proceedings paper. An image (shown left) of a single 100 mm FL lens configuration displaying 5 % of the 100,000 rays traced for visualization purposes. Shown in green is the current model featuring the parabolic mirror, flat mirror, LED and lens and shown in red are the rays the ray trace software simulated. Shown on the right is an example irradiance map generated from the ray trace using a 3.5 mm liquid light guide. The irradiance map shows rays incident on the liquid light guide using a 76.2 mm FL concave mirror and a 45 mm FL single lens configuration. [17]

2.2 Experimental Prototype

The optimized model was used to develop a prototype that utilized 12 different wavelength LEDs ranging from 365 nm to 525 nm. The prototype consisted of three main alignment plates: one plate holding the spherical mirror, another plate holding twelve 45 mm focal length lenses and the flat mirror, and the final plate holding a circuit board with twelve LEDs. The flat mirror and the lenses were combined into a single plate for simplicity. This was allowable due to the results from the optimization demonstrating an optimal distance over an optimal position.

The size of the 76.2 mm spherical mirror presented a problem with the number of lenses needed to fit in an annulus beneath it. A slightly smaller diameter (12.7 mm diameter as opposed to 15 mm diameter) 45 mm focal length lens was chosen to fit more LEDs and lenses in the annulus.

3.0 RESULTS

3.1 Theoretical Modeling Results

Results of the initial modeling optimization demonstrated a 76.2 mm focal length concave mirror with a 45 mm focal length lens yielded the highest optical transmission of 12%. These initial results were presented at Photonics West 2019 and a graph of the results for this configuration re-presented in Figure 3 to aid in comparison to the experimental prototype results. In Figure 3, optical transmission is graphed as a function of lens z position for various LED z positions. For each LED position there is an optimal distance from the lens where there is a peak transmission. Inferring from the graph as the LED is moved 10 increments the optimal position of the lens is moved 10 increments with no significant decrease in transmission seen after an LED z-position of 40.

Downloaded From: https://www.spiedigitallibrary.org/conference-proceedings-of-spie on 16 Mar 2020
Terms of Use: https://www.spiedigitallibrary.org/terms-of-use

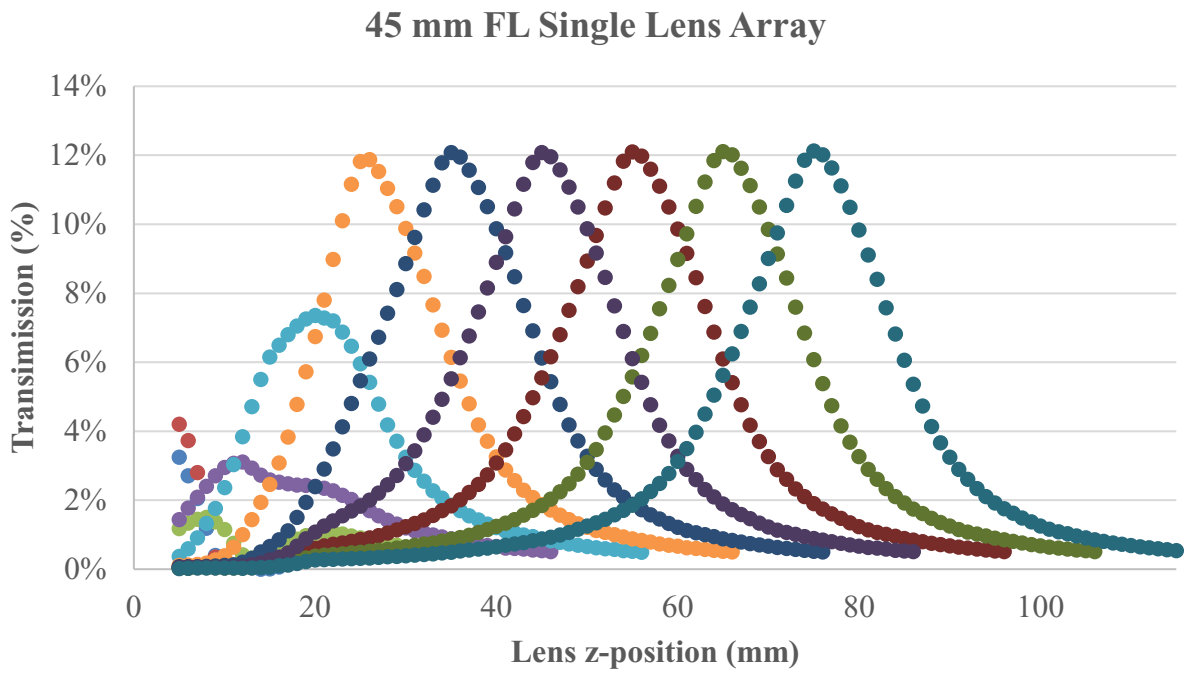

Figure 3 – Initial data is shown here for comparison from the previous year's proceedings paper. Graph of transmission vs. lens z-position for each LED z-position evaluated, using a 45 mm FL lens in a 76.2-mm FL concave mirror configuration from the ray trace model. The positions used are shown as relative to the origin in the model by distance of millimeters. Each different colored distribution on the graph represents a specific LED z-position, evaluated in increments of 10 mm. For each LED z-position the lens was moved in 1 mm increments starting at the top of the mirror and ending at the LED. Each point on the graph represents the percent transmission at each lens position for a specified LED position. [17]

3.2 Experimental Prototype Results

To produce similar data from the experimental prototype bench top testing: the three plates were anchored to optical translation stages that allowed for position tuning and the optical transmission was measured using an integrating sphere and fiber-coupled spectrometer (QE 65000, Ocean Optics, Inc.). The integrating sphere was located so as to receive the light exiting the liquid light guide. Optical transmission was calculated by dividing the liquid light guide output by the raw LED output. The integrating sphere was coupled to a spectrometer and illumination was measured directly from the source LED and from the exit of the liquid light guide. The LED used for testing was a 450 nm wavelength LED. The stages permitted movement of the LED plate and the spherical mirror plate in the two directions consistent with the model optimization, designated x (in a direction perpendicular to the long optical axis) and z (in a direction parallel to the optical axis). Optical throughput was measured in 1 mm increments for a range of 50 mm. The LED plate was adjusted in the z direction first. The LED z-position that obtained the highest throughput was then set, and data was acquired similarly for the mirror x and z plate. Finally, the LED plate was adjusted in the x-direction. Results from the testing of the LED z and x plate are shown in Figure 4. An optimal position was found for each plate and yielded an optical transmission of 1%.

Downloaded From: https://www.spiedigitallibrary.org/conference-proceedings-of-spie on 16 Mar 2020
Terms of Use: https://www.spiedigitallibrary.org/terms-of-use

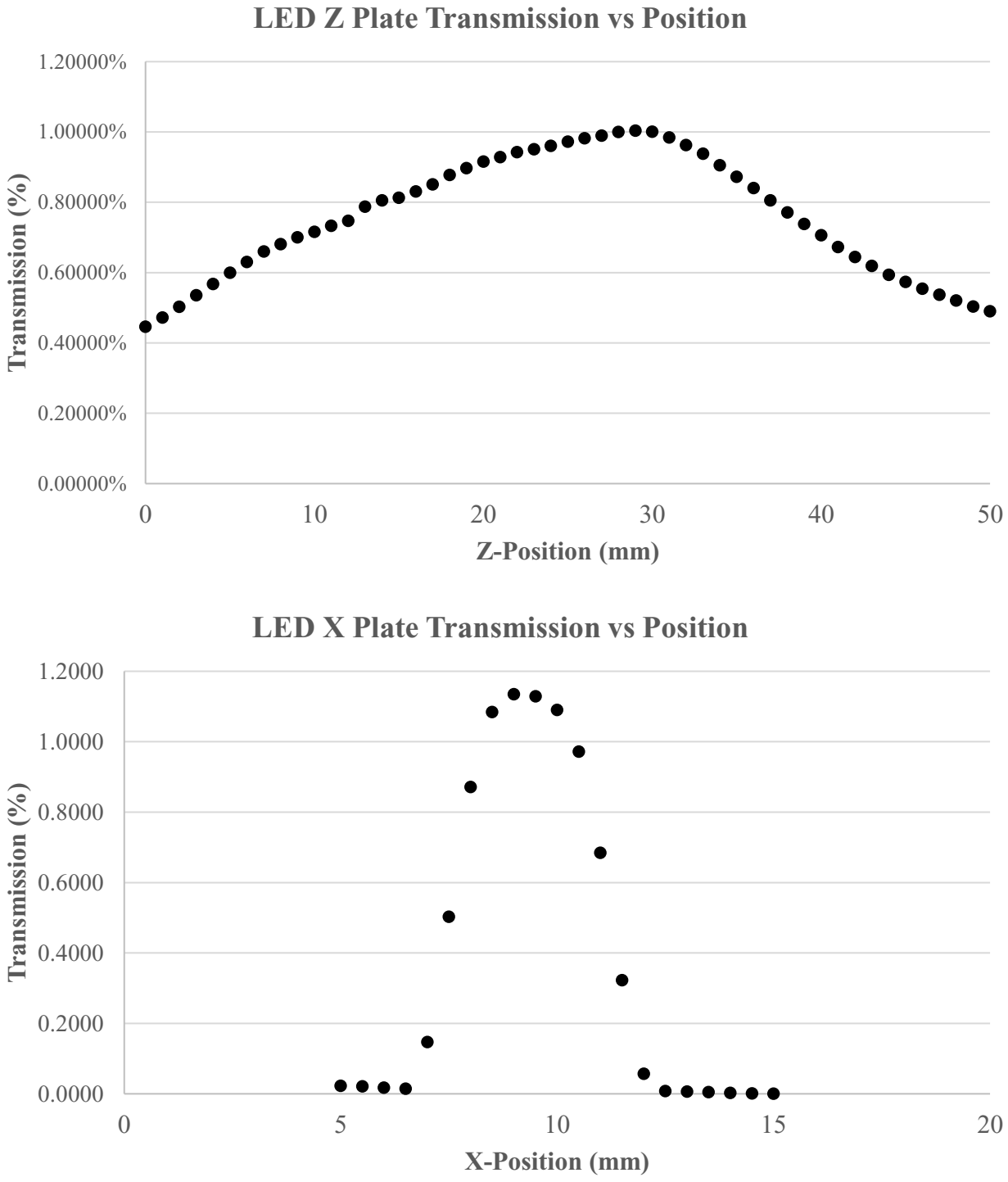

Figure 4 – Top) Graph of transmission vs. LED z-position measured experimentally on the prototype system for the LED plate using a 450 nm LED. The z-position of 0 mm is in reference to an arbitrary location at which the optical translation stage was attached to the optical bench. Bottom) Graph of transmission vs. LED x-position measured experimentally on the prototype system for the LED plate

Downloaded From: https://www.spiedigitallibrary.org/conference-proceedings-of-spie on 16 Mar 2020
Terms of Use: https://www.spiedigitallibrary.org/terms-of-use

using a 450 nm LED. The x-position of 5 mm is in reference to an arbitrary location at which the optical translation stage was attached to the optical bench.

4.0 FUTURE WORK

Future work will focus on optimizing the optical light path to increase optical transmission and coupling the prototype light source with a microscope to begin imaging.

5.0 ACKNOWLEDGEMENTS

The authors would like to acknowledge support from NIH Grants P01HL066299 and R01HL137030, NSF grant 1725937, and the Abraham Mitchell Cancer Research Fund. Drs. Leavesley and Rich disclose financial interest in a start-up company formed to commercialize spectral imaging technologies, SpectraCyte, LLC.

REFERENCES

[1] Young, M.R., "Principles and Technique of Fluorescence Microscopy," Journal of Cell Science s3-102(60), 419–449 (1961).

[2] Lakowicz, J.R., and Masters, B.R., "Principles of Fluorescence Spectroscopy, Third Edition," Journal of Biomedical Optics 13(2), 029901 (2008).

[3] Schultz, R.A., Nielsen, T., Zavaleta, J.R., Ruch, R., Wyatt, R., and Garner, H.R., "Hyperspectral imaging: A novel approach for microscopic analysis," Cytometry 43(4), 239–247 (2001).

[4] Zimmermann, T., Rietdorf, J., and Pepperkok, R., "Spectral imaging and its applications in live cell microscopy," FEBS letters 546(1), 87–92 (2003).

[5] Harris, A.T., "Spectral mapping tools from the earth sciences applied to spectral microscopy data," Cytometry Part A 69A(8), 872–879 (2006).

[6] Leavesley, S.J., Annamdevula, N., Boni, J., Stocker, S., Grant, K., Troyanovsky, B., Rich, T.C., and Alvarez, D.F., "Hyperspectral imaging microscopy for identification and quantitative analysis of fluorescently-labeled cells in highly autofluorescent tissue," Journal of Biophotonics 5(1), 67–84 (2012).

[7] Garini, Y., Young, I.T., and McNamara, G., "Spectral imaging: Principles and applications," Cytometry Part A 69A(8), 735–747 (2006).

[8] Li, Q., He, X., Wang, Y., Liu, H., Xu, D., and Guo, F., "Review of spectral imaging technology in biomedical engineering: achievements and challenges," Journal of Biomedical Optics 18(10), 100901 (2013).

[9] Lu, G., and Fei, B., "Medical hyperspectral imaging: a review," Journal of Biomedical Optics 19(1), 010901 (2014).

[10] Favreau, P.F., Hernandez, C., Heaster, T., Alvarez, D.F., Rich, T.C., Prabhat, P., and Leavesley, S.J., "Excitation-scanning hyperspectral imaging microscope," Journal of Biomedical Optics 19(4), 046010 (2014).

[11] Annamdevula, N.S., Sweat, B., Favreau, P., Lindsey, A.S., Alvarez, D.F., Rich, T.C., and Leavesley, S.J., "An Approach for Characterizing and Comparing Hyperspectral Microscopy Systems," Sensors 13(7), 9267–9293 (2013).

[12] Leavesley, S.J., Sweat, B., Abbott, C., Favreau, P., and Rich, T.C., "A theoretical-experimental methodology for assessing the sensitivity of biomedical spectral imaging platforms, assays, and analysis methods," Journal of Biophotonics 11(1), e201600227 (2018).

[13] Browning, C.M., Mayes, S., Rich, T.C., and Leavesley, S.J., "Design of a modified endoscope illuminator for spectral imaging of colorectal tissues," in Opt. Biopsy XV Real-Time Spectrosc. Imaging Diagn. 10060, 1006015 (2017).

Downloaded From: https://www.spiedigitallibrary.org/conference-proceedings-of-spie on 16 Mar 2020
Terms of Use: https://www.spiedigitallibrary.org/terms-of-use

[14] Mayes, S.A., Moore, K., Browning, C., Klomkaew, P., Rich, T.C., and Leavesley, S.J., "Applications and assessment of an excitation-scanning hyperspectral imaging system," in Imaging Manip. Anal. Biomol. Cells Tissues XVI 10497, 1049706 (2018).

[15] Leavesley, S.J., Walters, M., Lopez, C., Baker, T., Favreau, P.F., Rich, T.C., Rider, P.F., and Boudreaux, C.W., "Hyperspectral imaging fluorescence excitation scanning for colon cancer detection," Journal of Biomedical Optics 21(10), 104003 (2016).

[16] Deal, J., Mayes, S., Browning, C., Hill, S., Rider, P., Boudreaux, C., Rich, T., and Leavesley, S.J., "Identifying molecular contributors to autofluorescence of neoplastic and normal colon sections using excitation-scanning hyperspectral imaging," Journal of Biomedical Optics 24(2), 021207 (2018).

[17] Gunn Mayes, S., Mayes, S.A., Browning, C., Parker, M., Rich, T.C., and Leavesley, S.J., "A spherical mirror-based illumination system for fluorescence excitation-scanning hyperspectral imaging," in Imaging Manip. Anal. Biomol. Cells Tissues XVII, D. L. Farkas, J. F. Leary, and A. Tarnok, Eds., 22 (2019).

Downloaded From: https://www.spiedigitallibrary.org/conference-proceedings-of-spie on 16 Mar 2020
Terms of Use: https://www.spiedigitallibrary.org/terms-of-use